Atmos. Chem. Phys., 14, 8905–8915, 2014
www.atmos-chem-phys.net/14/8905/2014/
doi:10.5194/acp-14-8905-2014

Atmospheric Chemistry and Physics
Open Access

Air–sea exchange and gas–particle partitioning of polycyclic aromatic hydrocarbons in the Mediterranean

M. D. Mulder[1], A. Heil[2,*], P. Kukučka[1], J. Klánová[1], J. Kuta[1], R. Prokeš[1], F. Sprovieri[3], and G. Lammel[1,4]

[1]Masaryk University, Research Centre for Toxic Compounds in the Environment, Brno, Czech Republic
[2]Helmholtz Research Centre Jülich, Institute for Energy & Climate Research, Jülich, Germany
[3]CNR, Institute for Atmospheric Pollution Research, Rende, Italy
[4]Max Planck Institute for Chemistry, Mainz, Germany
[*]now at: Max Planck Institute for Chemistry, Mainz, Germany

Correspondence to: G. Lammel (lammel@recetox.muni.cz)

Received: 10 January 2014 – Published in Atmos. Chem. Phys. Discuss.: 6 March 2014
Revised: 24 July 2014 – Accepted: 25 July 2014 – Published: 1 September 2014

Abstract. Polycyclic aromatic hydrocarbon (PAH) concentration in air of the central and eastern Mediterranean in summer 2010 was 1.45 (0.30–3.25) ng m^{-3} (sum of 25 PAHs), with 8 (1–17) % in the particulate phase, almost exclusively associated with particles < 0.25 µm. The total deposition flux of particulate PAHs was 0.3–0.5 µ g m^{-2} yr^{-1}. The diffusive air–sea exchange fluxes of fluoranthene and pyrene were mostly found net-depositional or close to phase equilibrium, while retene was net-volatilisational in a large sea region. Regional fire activity records in combination with box model simulations suggest that seasonal depositional input of retene from biomass burning into the surface waters during summer is followed by an annual reversal of air–sea exchange, while interannual variability is dominated by the variability of the fire season. One-third of primary retene sources to the sea region in the period 2005–2010 returned to the atmosphere as secondary emissions from surface seawaters. It is concluded that future negative emission trends or interannual variability of regional sources may trigger the sea to become a secondary PAH source through reversal of diffusive air–sea exchange.

Capsule: In late summer the seawater surface in the Mediterranean has turned into a temporary secondary source of PAH, obviously related to biomass burning in the region.

1 Introduction

The marine atmospheric environment is a receptor for polycyclic aromatic hydrocarbons (PAHs) which are advected from combustion sources on land (power plants, biomass burning, road transport, domestic heating). Marine sources may be significant near transport routes (ship exhaust). Long-range transport from urban and industrial sources on land are the predominant sources of PAHs in the Mediterranean (Masclet et al., 1988; Tsapakis et al., 2003, 2006; Tsapakis and Stephanou, 2005a). A number of PAHs are semivolatile (vapour pressures at 298 K in the range 10^{-6}–10^{-2} Pa) and, hence, partition between the gas and particulate phases of the atmospheric aerosol, influenced by temperature, particulate-phase chemical composition and particle size (Keyte et al., 2013). Upon deposition to surface water, PAHs partition between the aqueous and particulate (colloidal and sinking) phases and may bioaccumulate in marine food chains (Lipiatou and Saliot, 1991; Dachs et al., 1997; Tsapakis et al., 2003; Berrojalbiz et al., 2011). They were also found enriched in the sea-surface microlayer relative to subsurface water (Lim et al., 2007; Guitart et al., 2010). Semivolatile PAHs may be subject to re-volatilisation from the sea surface (reversal of air–sea exchange), similar to chlorinated semivolatile organics (Bidleman and McConnell, 1995), in case high concentrations in surface water were to build up. This had been predicted by multicompartmental modelling for two–four-ring PAHs for polluted coastal waters and also the open ocean (Greenfield and Davis, 2005; Lammel et al., 2009a) and was

indeed observed in coastal waters off the northeastern United States (Lohmann et al., 2011). Field studies in the open sea found net deposition to prevail whenever determined (e.g. Tsapakis et al., 2006; Balasubramanian and He, 2010; Guitart et al., 2010; Castro-Jiménez et al., 2012; Mai, 2012). However, some three–four-ring parent PAHs – among them fluorene (FLN), fluoranthene (FLT) and pyrene (PYR) – were reported to be close to phase equilibrium in the Mediterranean, Black and North seas (Castro-Jiménez et al., 2012; Mai, 2012), and net volatilisation of FLT and PYR was observed in the open southeastern Mediterranean Sea in spring 2007 (Castro-Jiménez et al., 2012).

The aim of this study was to add insights on the cycling of PAHs in the Mediterranean in summer, with a focus on sources and phase partitioning in the aerosol.

2 Methods

2.1 Sampling

Gas- and particulate-phase air samples were taken during the RV *Urania* cruise, 27 August–12 September 2010 (Fig. S1 in the Supplement). The high-volume sampler (Digitel) was equipped with one glass fibre filter (GFF, Whatman) and one polyurethane foam (PUF) plug (Gumotex Břeclav, density 0.030 g cm^{-3}, 50 mm diameter, cleaned by extraction in acetone and dichloromethane, 8 h each, placed in a glass cartridge) in series. Particle size was classified in the particulate phase using high-volume filter sampling ($F = 68\,m^2\,h^{-1}$, model HVS110, Baghirra, Prague) and low-volume impactor sampling ($F = 0.54\,m^2\,h^{-1}$; Sioutas five-stage cascade; PM_{10} inlet, cutoffs 2.5, 1.0., 0.5 and 0.25 µm of aerodynamic particle size and back-up filter; impaction on quartz fibre filters (QFFs); SKC Inc., Eighty Four, USA; sampler Baghirra PM_{10-35}). In total 15 high-volume filter samples, exposed for 8–36 h (230–1060 m^3 of air), and 3 low-volume impactor samples, exposed for 5 days, were collected. Water sampling was performed using the stainless steel ROSETTE active sampling device equipped with 24 Niskin bottles (volume of 10 L) deployed in water at 1.5 m depth for surface water sampling.

PAH sampling on GFF and in PUF can be subject to losses related to oxidation of sorbed PAH by ozone (Tsapakis and Stephanou, 2003). This artefact is species-specific, and the more pronounced it is, the higher the ozone concentration and the longer the sampling time. Among the PAHs addressed, benzo(a)pyrene and pyrene have been identified as particularly vulnerable to oxidation. Based on such sampling artefact quantification studies (Tsapakis and Stephanou, 2003; Galarneau et al., 2006) and ozone levels (Table 1a) and sampling times (Table S1 in the Supplement), we expect that total PAHs are underestimated by up to 50 % in the gas phase and by up to 25 % in the particulate phase.

Table 1. Concentrations of PAHs found in (a) air (total, i.e. sum of gas and particulate phases, ng m^{-3}) and (b) seawater (total, i.e. sum of dissolved and particulate, ng L^{-1}) as time-weighted mean (min–max). n_{LOQ} represents number of samples > LOQ (out of 15 air and 23 seawater samples). PAHs with concentrations < LOQ in all samples not listed. For calculation of means, values < LOQ were replaced by LOQ/2. Ozone levels are given, too (ppbv).

(a)

	n_{LOQ}	mean (min–max)
ACE	4	0.025 (< 0.020–0.089)
FLN	10	0.137 (< 0.030–0.396)
PHE	15	0.581 (0.144–1.41)
ANT	13	0.043 (0.008–0.22)
RET	14	0.016 (0.006–0.030)
FLT	15	0.262 (0.053–0.795)
PYR	15	0.203 (0.044–0.564)
BAA	15	0.01 (0.0014–0.031)
CHR	15	0.04 (0.012–0.092)
TPH	15	0.018 (0.007–0.032)
BBN	11	0.018 (0.001– < 0.085)
BBF	15	0.021 (0.004–0.102)
BKF	14	0.012 (0.002– < 0.085)
BAP	12	0.015 (0.001– < 0.085)
BGF	15	0.021 (0.005–0.067)
CPP	7	0.012 (0.001– < 0.085)
BJF	15	0.016 (0.002–0.079)
BEP	14	0.019 (0.004–0.088)
PER	7	0.012 (0.001–0.1)
IPY	7	0.022 (0.008–0.094)
BPE	6	0.02 (0.009–0.085)
COR	5	0.016 (0.002–0.1)
Σ25 PAHs		1.539 (0.44–4.694)
Ozone		42 (33–65)

(b)

	n_{LOQ}	mean (min–max)
PHE	1	1.1
RET	12	0.1 (< 0.1–0.5)
FLT	10	0.1 (< 0.1–0.3)
PYR	7	0.2 (< 0.2–0.9)

With the aim to characterise the potential influences of ship-borne emissions on the samples, passive air samplers with PUF disks (150 mm diameter, 15 mm thick, deployed in protective chambers consisting of two stainless steel bowls; Klánová et al., 2008) were exposed at five different locations onboard during 16 days. The PAH levels of these samples indicated that ship-based contamination was negligible.

2.2 PAHs analyses and quality assurance

For PAH analysis all samples were extracted with dichloromethane in an automatic extractor (Büchi B-811). Surrogate recovery standards (D8-naphthalene,

D10-phenanthrene, D12-perylene) were spiked on each PUF and GFF prior to extraction. The volume was reduced after extraction under a gentle nitrogen stream at ambient temperature, and fractionation achieved on a silica gel column.

The extract was fractionated on a silica column (5 g of silica 0.063–0.200 mm, activated for 12 h at 150 °C). The first fraction (10 mL n-hexane) containing aliphatic hydrocarbons was discarded. The second fraction (20 mL dichloromethane) containing PAHs was collected and then reduced by stream of nitrogen in a TurboVap II (Caliper LifeSciences, USA) concentrator unit and transferred into an insert in a vial. Terphenyl was used as syringe standard; final volume was 200 µL. Gas-chromatography–mass-spectrometric (GC-MS) analysis was performed on a 6890N GC equipped with a 60 m × 0.25 mm × 0.25 µm DB5-MS column (Agilent J&W, USA) coupled to 5973N MS (Agilent, USA). The MS was operated in electron impact positive ion mode with selected ion recording (SIR). The targeted compounds are the 16 Environmental Protection Agency (EPA) priority PAHs (i.e. naphthalene (NAP), acenaphthylene (ACY), acenaphthene (ACE), fluorene (FLN), phenanthrene (PHE), anthracene (ANT), fluoranthene (FLT), pyrene (PYR), benzo(a)anthracene (BAA), chrysene (CHR), benzo(b)fluoranthene (BBF), benzo(k)fluoranthene (BKF), benzo(a)pyrene (BAP), indeno(1,2,3-cd)pyrene (IPY), dibenzo(ah)anthracene (DBA and benzo(ghi)perylene (BPE)), 10 more parent PAHs (i.e. benzo(ghi)fluoranthene (BGF), cyclopenta(cd)pyrene (CPP), triphenylene (TPH), benzo(j)fluoranthene (BJF), benzo(k)fluoranthene (BKF), benzo(e)pyrene (BEP), perylene (PER), dibenz(ac)anthracene (DCA), anthanthrene (ATT) and coronene (COR)) and 1 alkylated PAH, retene (RET). The injection volume was 1 µL. Terphenyl was used as the internal standard.

Field blank values, b, were gained from GFFs and PUFs manipulated in the field, as far as possible identical to the samples, except without switching the high-volume sampler on. No QFF field blank was taken for impactor sampling. As no PAHs were detected in the stages corresponding to 2.5–10 µm (all PAHs < limit of detection in all such samples), instead the mean of values of the QFF substrates of the two uppermost impactor stages (in total six) was taken. The respective b value was subtracted from sample values. The limit of quantification (LOQ) needs to take the accuracy of the blank level into account. Lacking a measure for the variation of the field blank, the relative standard deviation (SD) of field blanks from earlier field campaigns (σ_c / b_c) on a high-mountain site (high-volume sampling, summer 2007, $n = 5$; Lammel et al., 2009b) and in the Mediterranean (impactor sampling, summer 2008, $n = 6$; Lammel et al., 2010a) was used ($\sigma = (\sigma_c / b_c) \times b$). Identical samplers, sampling and analysis protocols for all analytes had been applied. Values below the sum of the field blank value (from this campaign) and three relative SDs of the field blank values (from the previous campaigns) were considered < LOQ (limit of quantification, $\mathrm{LOQ} = b + 3\sigma$). NAP and ACY were excluded from the data set because of the lack of blank values. The field blank values of most other analytes were below instrument LOQ in high-volume PUF and GFF samples. However, higher field LOQs, up to (6–25) pg m^{-3} (according to sampled volume of air), resulted for ANT, PYR and RET, and up to (45–180) pg m^{-3} for ACE, FLN, PHE and FLT in PUF. Field LOQs of PAHs in impactor QFF samples were below instrumental LOQ for most substances, but in the range (8–15) pg m^{-3} for ACE, ANT and FLT; ≈ 55 pg m^{-3} for FLN; and 120–140 pg m^{-3} for NAP and PHE.

The instrument LOQ, which is based on the lowest concentration of calibration standards used, was 0.5 ng, corresponding to 0.5–2.5 pg m^{-3} for high-volume samples, ≈ 8 pg m^{-3} for impactor samples, 6–10 pg m^{-3} for semivolatile PAHs determined in passive air samples and up to 200 pg m^{-3} for non-volatile PAHs in passive air samples.

Water samples (2–2.5 L) were extracted immediately after their collection using solid-phase extraction on C_{18} Empore disks using a vacuum manifold device. Disks were stored closed in glass vials in a freezer and transported to the processing laboratory; PAHs were eluted from disks using 40 mL of dichloromethane. The above-listed PAHs were analysed using GC-MS (Agilent GC 6890N coupled to an Agilent single quadrupole MS 5973N operating in electron impact ionisation mode). LOQ was 0.1 ng L^{-1}.

2.2.1 Other trace constituents and meteorological parameters

Ozone was measured with an absorption method (Teledyne–API model 400A UV) on the top deck (10 m above sea surface). Meteorological parameters (air temperature, humidity, wind direction and velocity) and oceanographic parameters were determined onboard.

2.3 Models of gas–particle partitioning

The data set (15 high-volume samples of separate gas- and particulate-phase concentrations) is used to test gas–particle partitioning models for semivolatile organics in terms of the organics' mass size distribution and size-dependent particulate matter (PM) composition. The models assume different processes to determine gas–particle partitioning, i.e. an adsorption model (Junge–Pankow; Pankow, 1987) and two absorption models (i.e. K_{OA} models; Finizio et al., 1997; Harner and Bidleman, 1998). Absorption is into particulate organic matter (OM). Adsorption to soot is a significant gas–particle partitioning processes for PAHs, but no soot data or PM chemical composition data are available. We, therefore, refrain from testing dual-adsorption and absorption models (e.g. Lohmann and Lammel, 2004). Particulate mass fraction, θ, and partitioning coefficient, K_p, are defined by the

concentrations in the two phases:

$$\theta = c_p/(c_p + c_g),$$
$$K_p = c_p/(c_g \times c_{TSP}) = \theta/[(1-\theta) \times c_{TSP}],$$

with PAH particulate- and gas-phase concentrations, c_p and c_g, in units of ng m^{-3}; c_p representing the whole particle size spectrum; and c_{TSP} representing concentration of total suspended matter.

Different models describe different processes to quantify differences in ad- and absorption between compounds. The Junge–Pankow (JP) model uses the vapour pressure of the sub-cooled liquid, p_L^0; $\theta = c_J\ S\ /\ (p_L^0 + c_J\ S)$ (data taken from Lei et al., 2002); and c_J should be approximately 171 Pa cm for PAHs (Pankow, 1987). The aerosol particle surface concentration, S, was not measured, and a typical value for maritime aerosols is adopted instead (4.32×10^{-7} cm^{-1}; Jaenicke, 1988). Harner and Bidleman (1998) use the $\log K_{OA}$ and f_{OM}: $\log K_p = \log K_{OA} + \log f_{OM} - 11.91$; Finizio et al. (1997) use only the K_{OA} as the predictor (data taken from Ma et al., 2010): $\log K_p = 0.79 \times \log K_{OA} - 10.01$. The range of the fraction of OM used here is based on Putaud et al. (2004) (16 % lower limit) and Spindler et al. (2012) (45 % upper limit).

2.4 Air–sea diffusive mass exchange calculations

State of phase equilibrium is addressed by fugacity calculation, based on the Whitman two-film model (Liss and Slater, 1974; Bidleman and McConnell, 1995**)**. The fugacity ratio (FR) is calculated as

$$FR = f_a\,/\,f_w = C_a RT_a\,/\,(C_w H_{Tw,\,salt}),$$

with fugacities from air and water f_a and f_w, gas-phase concentration C_a (ng m^3), dissolved aqueous concentration C_w (ng m^3), universal gas constant R (Pa m^3 mol^{-1} K^{-1}), water-temperature- and salinity-corrected Henry's law constant $H_{Tw,\,salt}$ (Pa m^3 mol^{-1}) and air temperature T_a (K). C_w is derived from the bulk seawater concentration, C_{bulk}:

$$C_w = C_{bulk}\,/\,(1 + K_{POC}C_{POC} + K_{DOC}C_{DOC}),$$

with particulate and dissolved organic carbon concentrations, C_{POC} and C_{DOC}, from Pujo-Pay et al. (2011) and K_{POC} and K_{DOC} from Karickhoff (1981), Lüers and ten Hulscher (1996), Rowe et al. (2009) and Ma et al. (2010). Values $0.3 < FR < 3.0$ are conservatively considered to not safely differ from phase equilibrium, as propagating from the uncertainty of the Henry's law constant, $H_{Tw,\,salt}$, and measured concentrations (e.g. Bruhn et al., 2003; Castro-Jiménez et al., 2012; Zhong et al., 2012). This conservative uncertainty margin is also adopted here, while $FR > 3.0$ indicates net deposition and $FR < 0.3$ net volatilisation. The diffusive air–seawater gas exchange flux (F_{aw}, ng m^{-2} day^{-1}) is calculated according to the Whitman two-film model (Bidleman and McConnell, 1995; Schwarzenbach et al., 2003):

$$F_{aw} = k_{ol}(C_w - C_a RT_a\,/\,H_{Tw,\,salt}),$$

with air–water gas exchange mass transfer coefficient (k_{ol}, m h^{-1}), accounting for resistances to mass transfer in both water (k_w, m h^{-1}) and air (k_a, m h^{-1}), defined as

$$1/k_{ol} = 1/k_w + RT_a/(k_a H_{Tw,\,salt}),$$

with $k_a = (0.2U_{10} + 0.3)\ \cdot\ (D_{i,air}/D_{H_2O,air})^{0.61} \times 36$ and $k_w = (0.45U_{10}^{1.64}) \times (Sc_i\,/\,Sc_{CO_2})^{-0.5} \times 0.01$. U_{10} is the wind speed at 10 m height above sea level (m s^{-1}), $D_{i,air}$ and $D_{H_2O,air}$ are the temperature-dependent diffusivities of substance i and H_2O in air, and Sc_i and Sc_{CO_2} are the Schmidt numbers for substance i and CO_2 (see Bidleman and McConnell, 1995; Zhong et al., 2012; and references therein). U_{10}, T_a, T_w and air pressure are taken from the ship-based measurements.

2.5 Non-steady-state two-box model

The air–sea mass exchange flux of RET is simulated by a non-steady-state zero-dimensional model of intercompartmental mass exchange (Lammel, 2004). RET is selected because of the prevalence of one dominating source. This two-box model predicts concentrations by integration of two coupled ordinary differential equations that solve the mass balances for the two compartments, namely the atmospheric marine boundary layer (MBL) and seawater surface mixed layer. Processes considered in air are dry (particle) deposition, removal from air by reaction with the hydroxyl radical and air–sea mass exchange flux (dry gaseous deposition); while in seawater export (settling) velocity, deposition flux from air, air–sea mass exchange flux (volatilisation) and degradation (as a first-order process) are considered. All input parameters are listed in Table S2 in the Supplement.

Atmospheric depositions related to emissions from open fires are assumed to provide the only source of seawater RET. These are available as daily time series for the eastern Mediterranean domain (28–45° N, 8–30° E) through the fire-related $PM_{2.5}$ emissions as provided by the Global Fire Assimilation System (GFASv1.0; Kaiser et al., 2012) in combination with an emission factor (207 mg RET in $PM_{2.5}$ (kg fuel burnt)$^{-1}$; Schmidl et al., 2008). The fire emissions are averaged over the domain and assumed to disperse within the MBL only. This is justified due to the assumed underestimation of the fire-related emissions and ignorance of other (emission) sources. The two-box model is run for the years 2005–2010, for the eastern Mediterranean domain (28–45° N, 8–30° E) with a 1 h time resolution. Air–sea mass exchange fluxes, F_{em}, in the range (0.30 ± 1.46) ng m^{-2} h^{-1} (positive defined upward) are simulated (using the initially estimated parameter set, Table S2 in the Supplement). GFAS uses global satellite observations of fire radiative power to estimate daily dry matter combustion rates and fire emission

fluxes. GFAS partly corrects for observational gaps (e.g. due to cloud cover) and detects fires in all biomes, except for very small fires (lower detection limit of around 100–1000 m^2 effective fire area).

2.6 Analysis of long-range advection of air

Distributions of potential sources can be identified by inverse modelling using meteorological input data (Stohl et al., 2003; Eckhardt et al., 2007). So-called retroplumes are generated using operational weather prediction model data and a Lagrangian particle dispersion model, FLEXPART (Stohl et al., 1998, 2005). Hereby, 50 000 virtual particles per hour were "released" and followed backwards in time for 5 days. The model output is a 3-D distribution of residence time.

3 Results and discussion

3.1 PAH concentrations in air and seawater

The mean total (i.e. sum of gaseous and particulate) Σ25 PAHs concentration is 1.45 ng m^{-3} (time-weighted; 1.54 with values < LOQ replaced by LOQ/2; see Table 1a), and ranged from 0.30 to 3.25 ng m^{-3}. The spatial variability of PAH levels in the Mediterranean is large, determined by long-range advection (Tsapakis and Stephanou, 2005a; Tsapakis et al., 2006). The levels found in this study in the southeastern Mediterranean (SEM) are for most substances lower than found earlier (Table 2). In the Ionian Sea and Sicily region (ISS) some PAHs are found somewhat higher than previously measured, i.e. FLT and PYR (in the gas phase) and BAP and PER (in the particulate phase). Due to a sampling artefact BAP and other particulate-phase PAHs could be underestimated by up to 25 % (aforementioned, Sect. 2.1). The seasonality of emissions and the variability of advection or advection in combination with different cruise routes being influenced differently by coastal or ship emission plumes can have a large influence and may explain these differences. On the other hand, the duration of temporal averaging atmospheric concentrations was similar across the various studies. Diagnostic ratios (BAA / (BAA + CHR), FLT / (FLT + PYR); Dvorská et al., 2011) in some of the samples (nos. 2, 4, 7, 8 and 15) reflect the influence of traffic and industrial sources. We investigated the potential source distribution of individual samples collected during the cruise (Sect. 2.6) and found that indeed maxima of PAH concentrations corresponded with air masses having resided over large urban areas, and, vice versa, low concentrations corresponded with air masses without apparent passage of such areas (illustrated in Fig. S4). This finding is supported by the ozone data, i.e. 53 (47–65) ppbv during influence from urban areas but 37 (33–62) ppbv otherwise.

It had been pointed out that the source distribution around the Mediterranean may cause a west–east gradient, leading to higher concentrations found in the ISS than in the SEM (Berrojalbiz et al., 2011). This gradient is somewhat reflected in our results, as levels in the ISS exceeded levels in the SEM (Table 2).

Most PAH concentrations in surface seawater were < LOQ, while FLT, PYR and RET were quantified in at least part of the samples (Table 1b). These observed seawater contamination levels are comparable to levels found in the region 2 and 1 decades ago (Lipiatou et al., 1997; Tsapakis et al., 2003). The concentrations near Crete (samples nos. 7 and 8a) are very similar to those found in fall 2001 and winter–spring 2002 (Tsapakis et al., 2006; FLT = 0.15 (0.11–0.21) ng L^{-1}, PYR = 0.12 (0.07–0.17) ng L^{-1}).

3.2 Gas–particle partitioning

Only a small mass fraction of the total, $\theta = 0.08$, is found in the particulate phase, confirming earlier findings from remote sites in the region (Tsapakis and Stephanou, 2005a; Tsapakis et al., 2006; Table 3c). The particulate mass fraction, θ, of four semivolatile PAHs varied considerably along the cruise track (see Fig. S2 in the Supplement). θ is thought to be strongly influenced by temperature, and doubling per 13 K cooling was found in a Mediterranean environment (Lammel et al., 2010b) apart from PM composition. We refrain from an exploration of the vapour pressure (p_L^0) dependence of θ (or K_p): a low time resolution implies lack of representativeness of the temperature measurement for the phase change (Pankow and Bidleman, 1992). Furthermore, non-equilibrium conditions cannot be excluded (but are likely as a consequence of time resolution; Hoff et al., 1998), and supporting physical and chemical aerosol parameters, necessary to relate to, are lacking. For similar temperatures higher θ values had been observed at sites in the region influenced by urban and industrial sources (Mandalakis et al., 2002; Tsapakis and Stephanou, 2005b; Akyüz and Çabuk, 2010), which is probably related to the influence of higher organic and soot PM mass fractions. Gas–particle partitioning models (Table 3) underpredict θ, except the Finizio et al. (1997) model for one substance, TPH. θ predicted by the JP model comes closest. A number of semivolatile PAHs could not be included in this test of gas–particle partitioning models as concentrations in either the gas phase (CPP, BBF, BJF) or the particulate phase (FLT, PYR, BBN) did not exceed LOQ or no insufficient input data were available (BBF). The neglect of adsorption to soot, not covered by the gas–particle partitioning models tested, may explain at least part of the underprediction (Lohmann and Lammel, 2004). Due to the lack of organic and elemental carbon data, an extended examination is not possible.

In size-segregated samples particulate PAH mass was almost exclusively found in the size fraction < 0.25 µm aerodynamic diameter (AD) (< LOQ in the other stages, except 0.002 ng m^{-3} CPP in the size fraction corresponding to 0.5-1.0 µm; Sect. S2.1 and Table S4 in the Supplement). Most particulate phase PAHs, 40 %, have been found associated

Table 2. Gaseous (a) and particulate (b) concentrations in air (time-weighted mean (min-max), ng m^{-3}) of selected PAHs compared to other studies in the Ionian Sea and Sicily region (ISS) and in the southeastern Mediterranean (SEM). For calculation of means, values < LOQ were replaced by LOQ/2. RV represents research vessel cruise.

(a)

	ISS		SEM			
	RV August–September 2010	RV June 2006, May 2007	RV August–September 2010	RV June 2006, May 2007	Finokalia September–October 2001, February, March and July 2002[1]	Finokalia November 2000–February 2002[2]
	This study	Castro-Jiménez et al. (2012)	This study	Castro-Jiménez et al. (2012)	Tsapakis et al. 2006	Tsapakis and Stephanou (2005a)
FLN	0.16 (< 0.027–0.34)	2.25 (1.27–5.65)	0.071 (< 0.050–0.40)	0.69 (0.36–1.23)	1.05 (0.15–1.67)	1.8 (0.2–5.7)
PHE	0.52 (0.14–1.11)	7.00 (3.52–15.45)	0.35 (0.14–1.41)	3.94 (2.50–6.35)	4.78 (1.75–7.78)	7.3 (1.5–27.7)
ANT	0.040 (< 0.021–0.10)	0.37 (0.18–0.55)	0.039 (< 0.013–0.22)	0.20 (0.16–0.30)	0.61 (0.12–1.31)	0.9 (0.1–4.5)
FLT	0.14 (0.053–0.31)	0.05 (0.02–0.07)	0.10 (0.061–0.37)	0.007 (0.003–0.011)	0.82 (0.12–1.69)	1.8 (0.07–6.0)
PYR	0.14 (0.058–0.56)	0.04 (0.02–0.06)	0.12 (0.044–0.29)	0.006 (0.003–0.009)	0.65 (0.14–0.97)	0.9 (0.1–2.8)
CHR	0.012 (0.0071–0.021)	0.09 (0.03–0.23)	0.014 (0.012–0.037)	0.03 (0.02–0.05)	0.18 (0.06–0.33)	0.2 (< 0.001–0.6)
Sum of 6 PAHs	1.0	9.8	0.7	4.9	8.1	12.9

(b)

	ISS		SEM		
	RV August–September 2010	RV June 2006, May 2007	RV August–September 2010	RV June 2006, May 2007	Finokalia November 2000–February 2002
	This study	Castro-Jiménez et al. (2012)	This study	Castro-Jiménez et al. (2012)	Tsapakis & Stephanou (2005a)
FLN	< 0.92 (< 0.60–< 1.1)	0.001 (0.0009–0.002)	< 0.66 (< 0.33–< 1.4)	0.0013 (0.0011–0.0016)	0.02 (< 0.001–0.01)
PHE	< 1.9 (< 1.2–< 2.3)	0.06 (0.01–0.12)	< 1.6 (< 0.66–< 2.7)	0.04 (0.01–0.13)	0.05 (0.004–0.2)
ANT	< 0.21 (< 0.14–< 0.26)	0.007 (0.0009–0.012)	< 0.16 (< 0.07–< 0.32)	0.009 (0.0007–0.023)	0.004 (< 0.001–0.02)
FLT	< 0.85 (< 0.56–< 1.0)	0.099 (0.01–0.19)	< 0.62 (< 0.30–< 1.3)	0.049 (0.01–0.12)	0.1 (0.04–0.2)
PYR	< 0.11 (< 0.070–< 0.13)	0.109 (0.016–0.216)	< 0.08 (< 0.044–< 0.16)	0.057 (0.012–0.142)	0.04 (0.01–0.01)
BAA	0.0054 (< 0.0018–0.025)	0.013 (0.006–0.023)	0.0026 (< 0.0006–0.0080)	0.018 (0.004–0.046)	0.03 (0.003–0.1)
CHR	0.018 (0.0030–0.076)	0.04 (0.01–0.08)	0.0079 (0.0033–0.020)	0.043 (0.012–0.101)	0.1 (0.02–0.3)
BBF	0.023 (< 0.0018–0.010)	0.029 (0.012–0.045)	0.011 (0.0042–0.033)	0.033 (0.010–0.060)	0.04 (< 0.001–0.2)
BKF	0.012 (< 0.0018–0.057)	0.015 (0.005–0.027)	0.0047 (0.0018–0.015)	0.089 (0.005–0.333)	0.04 (< 0.001–0.2)
BAP	0.013 (< 0.0009–0.072)	0.009 (0.04–0.016)	0.0046 (< 0.0011–0.0098)	0.034 (0.005–0.081)	0.02 (0.01–0.05)
BJF	0.018 (< 0.0018–0.079)	0.015 (0.014–0.016)	0.0072 (0.0023–0.031)	0.010 (0.008–0.011)	–
BEP	0.019 (< 0.0018–0.088)	0.03 (0.02–0.05)	0.0082 (0.0035–0.025)	0.046 (0.017–0.093)	0.04 (0.01–0.1)
PER	0.0023 (< 0.00096–0.011)	0.002 (0.0005–0.004)	0.00075 (< 0.0006–0.0021)	0.026 (0.0001–0.068)	0.004 (< 0.001–0.01)
IPY	0.015 (< 0.00096–0.094)	0.018 (0.006–0.032)	0.0016 (< 0.00052–0.019)	0.009 (0.002–0.013)	0.03 (0.009–0.2)
BPE	< 0.0014 (< 0.00096–0.0018)	0.026 (0.017–0.042)	0.0041 (< 0.00052–0.020)	0.081 (0.012–0.210)	0.03 (0.010–0.09)
Sum of 15 PAHs	0.09	1.06	0.05	0.54	0.54

[1] months September and October 2001, February, April and May 2002. No particulate data reported.
[2] 24 h per month between February 2000 and February 2002.

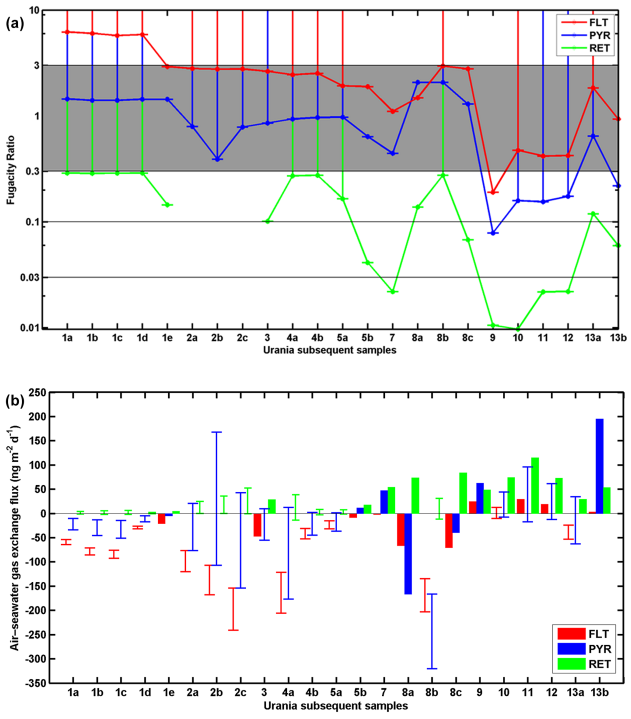

Figure 1. Air–sea exchange, **(a)** fugacity ratios FR = f_a / f_w (volatilisation > 3, deposition < 0.3, grey area insignificant deviation from phase equilibrium) and **(b)** flux F_{aw} (ng m^{-2} d^{-2}; volatilisation > 0, deposition < 0) of FLT, PYR and RET during the cruise of RV *Urania*. Error bars indicate sea water concentration C_w < LOQ. The *x* axis depicts the correspondence of sequential pairs of air samples (1–13) and water samples **(a–e)**.

with particles < 0.5 µm out of five size ranges in the marine background aerosol of the sea region (coast of Crete, November 1996–June 1997; Kavouras and Stephanou, 2002). At continental sites in central and southern Europe mass median diameters of PAHs were found to be in the accumulation range, mostly 0.5–1.4 µm (Schnelle et al., 1995; Kiss et al., 1998; Lammel et al., 2010b, c), but also a second, coarse mode was found (up to 2.4 µm; Chrysikou et al., 2009).

3.3 Fugacity ratio and air–sea exchange flux

Fugacity ratios (Fig. 1a) and vertical fluxes (Fig. 1b) could be quantified for FLT, PYR and RET. The uncertainty window of FR = f_a / f_w = 0.3–3.0 is based on the uncertainty of $H_{Tw,\,salt}$. Values of FR > 3.0 indicate net deposition; values of FR < 0.3 indicate net volatilisation. For RET both water and air concentrations of sample no. 2 were < LOQ. Transfer coefficients were $k_w \ll k_a$.

FLT and PYR were found to be close to phase equilibrium, with most of the FR values within the uncertainty range, one sample (no. 1) indicating deposition of FLT and one or two (nos. 9 and 13) indicating volatilisation of FLT and PYR, respectively. In comparison with earlier observations of FLT and PYR air–sea exchange in the SEM in 2001–2002 and 2007 (Tsapakis et al., 2006; Castro-Jiménez et al., 2012) and considering spatial and temporal variabilities, no trend – in particular no reversal of air–sea exchange – is indicated. This comparison is detailed in the Supplement, Sect. 2.2.1. RET, however, is found to be net-volatilisational throughout most of the cruise (Fig. 1). Among the highest fluxes (> 50 ng m^2 d^{-1}) are some samples with very low FR, < 0.03. Fugacity of RET from water is supported by its Henry's law coefficient (11 Pa m^3 mol^{-1} at 298 K), which is higher than for CHR (0.53 Pa m^3 mol^{-1}) and FLT (2.0 Pa m^3 mol^{-1}). RET is commonly considered a biomarker for coniferous wood combustion (Ramdahl, 1983). A decrease in wildfires could explain the suspected RET volatilisation. Integrated over the domain and the year 2010, fires released 7.2 PJ fire radiative energy, which translates into around 22.2 Gg of $PM_{2.5}$ emitted (Fig. 2). Compared to the $PM_{2.5}$ emissions of the years 2003 to 2012, the year 2010 had the lowest emissions, equivalent to 46 % of the 2003–2012 mean, and only 18 % of the peak emissions of the year 2007 (Fig. 2d). As is typical for the eastern Mediterranean region, the fire season in 2010 started by the end of June and ended by early October. The *Urania* cruise measurements took place between 27 August and 12 September, i.e. towards the end of the main burning season (Fig. 2c). During the first half of the *Urania* cruise, widespread fire activity was observed in the entire domain, with most intense fires occurring in southern Italy, Sicilia and along the east coast of the Adriatic and the Ionian Sea (notably in Albania and Greece) (Fig. 2a).

The hypothesis that seasonal depositional input of RET into the surface waters during the fire season (summer) triggers reversal of diffusive air–sea exchange, at least in the year 2010, is tested by box model (Sect. 2.5 and Sect. S1.3 in the Supplement) runs. Two scenarios are considered, an "initially estimated parameter set" (IEPS) representing mean values for environmental parameters, and an "upper estimate parameter set" (UEPS) which represents realistic environmental conditions favouring seawater pollution (Table S3 in the Supplement). Simulated diffusive air–sea exchange flux, F_{aw}, during 2005–2010 initialised by the UEPS is shown in Fig. 3a, initialised by the IEPS in Fig. S3 in the Supplement and initialised by the UEPS during the observations (cruise of RV *Urania*, 27 August–9 September 2010) in Fig. 3b.

The model confirms the hypothesis that seasonal depositional input of RET into the surface waters during the fire season (July–September, typically in the range $F_{aw} = 10^{-2}$–10^{1} ng m^{-2} d^{-1} under IEPS) is followed by a period of prevailing flux reversal, typically $F_{aw} = 10^{-2}$–10^{0} ng m^{-2} d^{-1}, which in the years 2008–2010 started in October and lasted until the onset of the fire season, but possibly started later in the years 2005–2007 (at least under IEPS). The volatilisation flux is predicted to be smaller in magnitude than the net-deposition flux during the fire season, but correspondingly, i.e. higher after intense fire seasons. The high RET volatilisation flux, indicated by measured C_a and C_w, seems to be

Table 3. Gas–particle partitioning of selected PAHs (mean ± SD (median)), observed and predicted by the models Junge–Pankow (1987) (JP), Harner and Bidleman (1998) (HB) and Finizio et al. (1997) (F), expressed as (a) particulate mass fraction, θ, and (b) log K_p of this study.

	Observed	JP	HB	F
(a)				
BAA	0.51 ± 0.28 (0.47)	0.18 ± 0.07 (0.18)	0.08–0.20	0.18
TPH	0.27 ± 0.13 (0.26)	0.24 ± 0.10 (0.24)	0.23–0.46	0.37
CHR	0.35 ± 0.15 (0.35)	0.31 ± 0.13 (0.32)	0.09–0.21	0.19
BBF	0.88 ± 0.40 (0.94)	0.91 ± 0.40 (0.97)	0.49–0.73	0.59
(b)				
BAA	−1.28 ± 1.00 (−0.96)	−1.97 ± 1.14 (−1.84)	2.43– −1.98	−1.89
TPH	−1.77 ± 1.27 (1.45)	−1.80 ± 1.07 (−1.63)	−1.91– −1.46	−1.48
CHR	−1.59 ± 1.18 (1.34)	−1.65 ± 1.01 (−1.46)	−2.41– −1.96	−1.87
BBF	−0.94 ± 0.19 (−0.24)	−0.52 ± 0.66 (−0.74)	−1.41– −0.96	−1.08

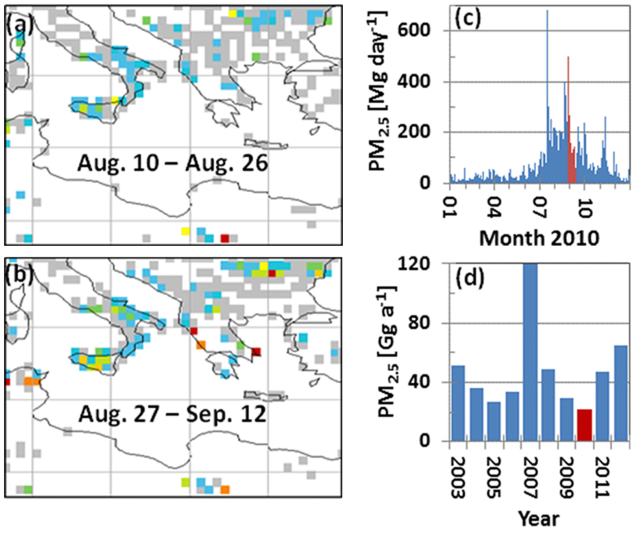

Figure 2. Spatial pattern of fire-related $PM_{2.5}$ emissions (Global Fire Assimilation System, GFASv1.0; Kaiser et al., 2012) for the eastern Mediterranean (28–45° N/8–30° E), **(a)** time integral of 10–26 August, **(b)** time integral of 27 August–12 September 2010, given as sum over each period in metres per milligram. Areas with no observed fire activity are displayed in white. Temporal pattern of domain-integrated **(c)** daily total $PM_{2.5}$ emissions over 2010 **(c)** and yearly total $PM_{2.5}$ emissions over 2003 to 2012. Labelled in red is **(c)** the the period of the *Urania* cruise (27 August–11 September 2010) and **(d)** the year 2010.

dominated by biomass burning in the region in the previous fire season. F_{aw} is predicted to be highly fluctuating, also during the observational period (Fig. 3b). Even under UEPS the model underpredicts F_{aw} (Fig. 3b). The sensitivity to input uncertainties (Sect. S1.2 in the Supplement) may explain part of the underestimate, but not up to 1 order of magnitude. Neglected RET sources to seawater, such as riverine input, may explain part of the discrepancy.

4 Conclusions

PAH pollution of the atmospheric Mediterranean environment was below previous observations at the beginning of the decade (2001–2002; Tsapakis and Stephanou, 2005a; Tsapakis et al., 2006), also considering possible losses during sampling. This might reflect emission reductions. The particulate-phase PAHs were concentrated in the size fraction < 0.25 µm AD. The residence time in the troposphere is longest for particles around 0.2 µm in size, with ≈ 0.01 cm s^{-1} being a characteristic corresponding dry deposition velocity (Franklin et al., 2000), which translates into a residence time of ≈120 days in the MBL (depth of 1000 m; see Table S3 in the Supplement) and deposition flux $F_{dep} = c \times v = 0.03$–$0.06$ µg m^{-2} yr^{-1} for the individual PAHs associated with the particulate phase ($c = 0.01$–0.02 ng m^{-3}; Table 2b), such as BAP, and 0.5 and 0.3 µg m^{-2} yr^{-1}, respectively, for the total flux of particulate phase PAHs in the ISS and SEM in summer. The flux will be higher in winter because of the seasonality of the emissions.

Three gas–particle partitioning models were tested and found to underpredict the particulate mass fraction in most of the samples (four PAHs, i.e. BAA, TPH, CHR and BBF). Although input parameters were incomplete, these results confirm the earlier insight that additional processes on the molecular level need to be included, beyond adsorption (Junge–Pankow model) and absorption in OM (K_{oa} models), namely both adsorption and absorption (Lohmann and Lammel, 2004) or even a complete description of molecular interactions between sorbate and PM matrix (Goss and Schwarzenbach, 2001).

Simulations with a non-steady-state two-box model confirm the hypothesis that seasonal depositional input of RET from biomass burning into the surface waters during summer is followed by a period of flux reversal. The volatilisation flux is smaller in magnitude than the net-deposition

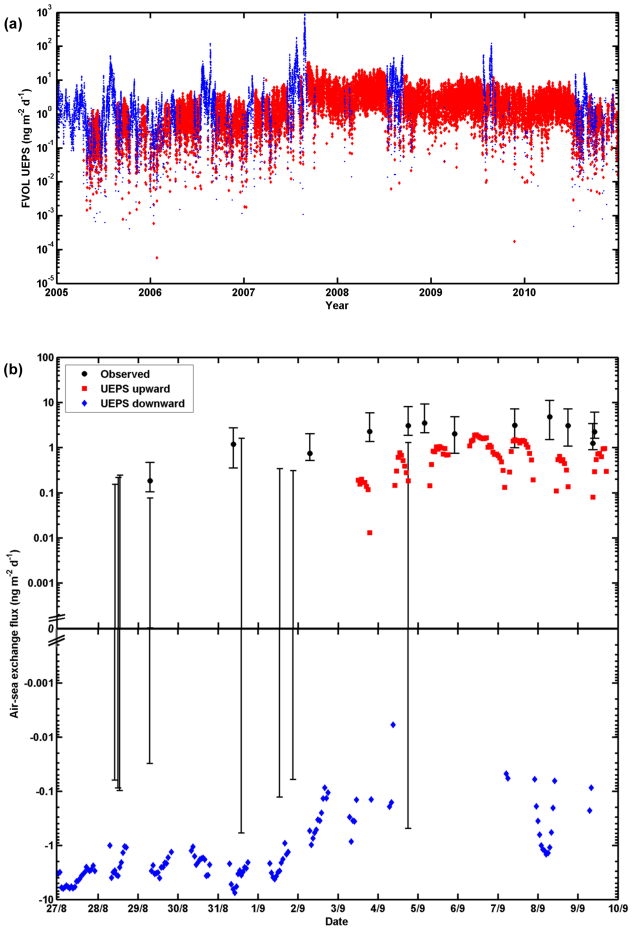

Figure 3. Diffusive air–sea exchange flux, F_{aw}, of RET (ng m^{-2} d^{-1}; downward in blue and upward in red) using the upper estimate parameter set (UEPS) for the eastern Mediterranean (28–45° N/8–30° E) **(a)** model predicted for 1 January 2005–31 December 2010 and **(b)** model predicted and observed (black) for 27 Author–9 September 2010. Hourly mean data filtered against offshore winds (see text). Error bars including both signs of F_{aw} reflect C_w < LOQ.

flux during the previous months, but correspondingly, i.e. higher after intense fire seasons. Future negative emission trends or interannual variability of regional sources may trigger the sea to become a secondary PAH source through reversal of diffusive air–sea exchange. For the wood burning marker RET, it is found that the secondary source has become significant in recent years: while the flux of secondary RET emissions (from surface seawaters) in the study area was 1.0 µg m^{-2} yr^{-1} (mean of years 2005–2010, _UEPS), the primary sources amounted to 3.1 µg m^{-2} yr^{-1}. Because of non-diffusive emission from the sea surface, such as aerosol suspension from sea spray and bubble bursting (Woolf, 1997; Qureshi et al., 2009; Albert et al., 2012), the true volatilisation may have exceeded the diffusive flux significantly.

The Supplement related to this article is available online at doi:10.5194/acp-14-8905-2014-supplement.

Acknowledgements. We thank the crew of RV *Urania* for scientific support during the cruise, and Giorgos Kouvarakis and Nikolaos Mihalopoulos (University of Crete) Franz Meixner (MPIC) and Manolios Tsapakis (HCMR Gournes-Pediados), for discussion and providing meteorological data. This research was supported by the Granting Agency of the Czech Republic (GACR project no. P503/11/1230) and by the European Commission (European Structural Funds project no. CZ.1.05/2.1.00/01.0001, CETOCOEN), and it was co-funded by the European Social Fund and the state budget of the Czech Republic.

Edited by: W. Maenhaut

References

Akyüz, M. and Çabuk, H.: Gas-particle partitioning and seasonal variation of polycyclic aromatic hydrocarbons in the atmosphere of Zonguldak, Turkey, Sci. Total Environ., 408, 5550–5558, 2010.

Albert, M. F. M. A., Schaap, M., Manders, A. M. M., Scannell, C., O'Dowd, C. D., and de Leeuw, G.: Uncertainties in the determination of global sub-micron marine organic matter emissions, Atmos. Environ., 57, 289–300, 2012.

Balasubramanian, R. and He, J.: Fate and transfer of persistent organic pollutants in a multimedia environment, edited by: Zereini, F., Wiseman, C. L. S., in: Urban airborne particulate matter: origins, chemistry, fate and health impacts. Springer, Heidelberg, 277–307, 2010.

Berrojalbiz, N., Dachs, J., Ojeda, M. J., Valle, M. C., Castro Jiménez, J., Wollgast, J., Ghiani, M., Hanke, G., and Zaldivar, J. M.: Biogeochemical and physical controls on concentrations of polycyclic aromatic hydrocarbons in water and plankton of the Mediterranean and Black Seas, Global Biogeochem. Cy., 25, GB4003, doi:10.1029/2010GB003775, 2011.

Bidleman, T. F. and McConnell, L. L.: A review of field experiments to determine air–water gas-exchange of persistent organic pollutants, Sci. Total Environ., 159, 101–107, 1995.

Bruhn, R., Lakaschus, S., and McLachlan, M. S.: Air/sea gas exchange of PCBs in the southern Baltic sea, Atmos. Environ., 37, 3445–3454, 2003.

Castro-Jiménez, J., Berrojalbiz, N., Wollgast, J., and Dachs, J.: Polycyclic aromatic hydrocarbons (PAHs) in the Mediterranean Sea: Atmospheric occurrence, deposition and decoupling with settling fluxes in the water column, Environ. Pollut., 166, 40–47, 2012.

Chrysikou, L. P., Gemenetzis, P. G., and Samara, C. A.: Wintertime size distributions of polycyclic aromatic hydrocarbons (PAH). polychlorinated biphenyls (PCB) and organochlorine pesticides (OCPs) in the urban environment: Street- vs. rooftop-level measurements. Atmos. Environ., 43, 290–300, 2009.

Dachs, J., Bayona, J. M., Raoux, C., and Albaiges, J.: Spatial, vertical distribution and budget of polycyclic aromatic hydrocarbons in the western Mediterranean seawater, Environ. Sci. Technol., 31, 682–688, 1997.

Dvorská, A., Lammel, G., and Klánová, J.: Use of diagnostic ratios for studying source apportionment and reactivity of ambient polycyclic aromatic hydrocarbons over central Europe. Atmos. Environ., 45, 420–427, 2011.

Eckhardt, S., Breivik, K., Manø, S., and Stohl, A.: Record high peaks in PCB concentrations in the Arctic atmosphere due to long-range transport of biomass burning emissions, Atmos. Chem. Phys., 7, 4527–4536, doi:10.5194/acp-7-4527-2007, 2007.

Finizio, A., Mackay, D., Bidleman, T. F., and Harner, T.: Octanol-air partition coefficient as a predictor of partitioning of semi-volatile organic chemicals to aerosols, Atmos. Environ., 31, 2289–2296, 1997.

Franklin, J., Atkinson, R., Howard, P. H., Orlando, J. J., Seigneur, C., Wallington, T. J., and Zetzsch, C.: Quantitative determination of persistence in air. In: Criteria for persistence and long-range transport of chemicals in the environment, edited by: Klečka, G., Boethling, B., Franklin, J., Grady, L., Graham, D., Howard, P. H., Kannan, K., Larson, R. J., Mackay, D., Muir, D., van de Meent, D., SETAC Press, Pensacola, USA, 7–62, 2000.

Galarneau, E., Bidleman, T. F., and Blanchard, P.: Modelling the temperature-induced blow-off and blow-on artefacts in filter-sorbent measurements of semivolatile substances, Atmos. Environ., 40, 4258–4268, 2006.

Goss, K. U. and Schwarzenbach, R. P.: Linear free energy relationships used to evaluate equilibrium partitioning of organic compounds, Environ. Sci. Technol., 35, 1–9, 2001.

Greenfield, B. K. and Davis, J. A.: A PAH fate model for San Francisco Bay, Chemosphere, 6, 515–530, 2005.

Guitart, C., Garcá-Flor, N., Miquel, J. C., Fowler, S. W., and Albaíges, J.: Effect of accumulation PAHs in the sea surface microlayer on their coastal air-sea exchange, J. Mar. Syst., 79, 210–217, 2010.

Harner, T. and Bidleman, T. F.: Octanol–air partition coefficient for describing particle-gas partitioning of aromatic compounds in urban air, Environ. Sci. Technol., 32, 1494–1502, 1998.

Hoff, E. M., Brice, K. A., and Halsall, C. J.: Non-linearities in the slope of Clausius-Clapeyron plots for semivolatile organic compounds, Environ. Sci. Technol., 32, 1793–1798, 1998.

Jaenicke, R.: Aerosol physics and chemistry., in: Numerical Data and Functional Relationships in Science and Technology, edited by: Fischer, G., 4, 391–457, Springer, Berlin, 1988.

Kaiser, J. W., Heil, A., Andreae, M. O., Benedetti, A., Chubarova, N., Jones, L., Morcrette, J. J., Razinger, M., Schultz, M. G., Suttie, M., and van der Werf, G. R.: Biomass burning emissions estimated with a global fire assimilation system based on observed fire radiative power, Biogeosciences, 9, 527–554, doi:10.5194/bg-9-527-2012, 2012.

Karickhoff, S. W.: Semiempirical estimation of sorption of hydrophobic pollutants on natural sediments and soils, Chemosphere, 10, 833–849, 1981.

Kavouras, I. G. and Stephanou, E. G.: Particle size distribution of organic primary and secondary aerosol constituents in urban, background marine, and forest atmosphere, J. Geophys. Res., 107, 4069, doi:10.1029/2000JD000278, 2002.

Keyte, I. J., Harrison, R. M., and Lammel, G.: Chemical reactivity and long-range transport potential of polycyclic aromatic hydrocarbons – a review, Chem. Soc. Rev., 42, 9333–9391, 2013.

Kiss, G., Varga-Puchony, Z., Rohrbacher, G., and Hlavay, J.: Distribution of polycyclic aromatic hydrocarbons on atmospheric aerosol particles of different sizes, Atmos. Res., 46, 253–261, 1998.

Klánová, J., Čupr, P., Kohoutek, J., and Harner, T.: Assessing the influence of meteorological parameters on the performance of polyurethane foam-based passive air samplers, Environ. Sci. Technol., 42, 550–555, 2008.

Lammel, G.: Effects of time-averaging climate parameters on predicted multicompartmental fate of pesticides and POPs, Environ. Pollut., 128, 291–302, 2004.

Lammel, G., Sehili, A. M., Bond, T. C., Feichter, J., and Grassl, H.: Gas/particle partitioning and global distribution of polycyclic aromatic hydrocarbons – a modelling approach, Chemosphere, 76, 98–106, 2009a.

Lammel, G., Klánová, J., Kohoutek, J., Prokeš, R., Ries, L., and Stohl, A.: Observation and origin of organochlorine pesticides, polychlorinated biphenyls and polycyclic aromatic hydrocarbons in the free troposphere over central Europe, Environ. Pollut., 157, 3264–3271, 2009b.

Lammel G., Klánová J., Ilić P., Kohoutek J., Gasić B., Kovacić I., Lakić N., and Radić R.: Polycyclic aromatic hydrocarbons on small spatial and temporal scales – I. Levels and variabilities, Atmos. Environ., 44, 5015–5021, 2010a.

Lammel, G., Klánová, J., Ilić, P., Kohoutek, J., Gasić, B., Kovacić, I., and Škrdlíková, L.: Polycyclic aromatic hydrocarbons on small spatial and temporal scales – II. Mass size distributions and gas-particle partitioning, Atmos. Environ., 44, 5022–5027, 2010b.

Lei, Y. D., Chankalal, R., Chan, A., and Wania, F.: Supercooled liquid vapor pressures of the polycyclic aromatic hydrocarbons, J. Chem. Eng. Data, 47, 801–806, 2002.

Lim, L., Wurl, O., Karuppiah, S., and Obbard, J. P.: Atmospheric wet deposition of PAHs to the sea-surface microlayer, Mar. Poll. Bull., 54, 1212–1219, 2007.

Lipiatou, E. and Saliot, A.: Fluxes and transport of anthropogenic and natural polycyclic aromatic-hydrocarbons in the western Mediterranean Sea, Mar. Chem., 32, 51–71, 1991.

Lipiatou, E., Tolosa, I., Simó, R., Bouloubassi, I., Dachs, J., Marti, S., Sicre, M. A., Bayona, J. M., Grimalt, J. O., Saliott, A., and Albaiges J.: Mass budget and dynamics of polycyclic aromatic hydrocarbons in the Mediterranean Sea, Deep Sea Res. II, 44, 881–905, 1997.

Liss, P. S. and Slater, P. G.: Flux of gases across air–sea interface, Nature, 247, 181–184, 1974.

Lohmann, R. and Lammel G.: Adsorptive and absorptive contributions to the gas particle partitioning of polycyclic aromatic hydrocarbons: State of knowledge and recommended parameterization for modelling, Environ. Sci. Technol., 38, 3793–3803, 2004.

Lohmann, R., Dapsis, M., Morgan, E. J., Dekany, E., and Luey, P. J.: Determining airwater exchange spatial and temporal trends of freely dissolved PAHs in an urban estuary using passive polyethylene samplers. Environ. Sci. Technol., 45, 2655–2662, 2011.

Lüers, F. and ten Hulscher, T. E. M.: Temperature effect on the partitioning of polycyclic aromatic hydrocarbons between natural organic carbon and water, Chemosphere, 33, 643–657, 1996.

Ma, Y. G., Lei, Y. D., Xiao, H., Wania, F., and Wang, W. H.: Critical review and recommended values for the physical-chemical

property data of 15 polycyclic aromatic hydrocarbons at 25 °C, J. Chem. Eng. Data, 55, 819–825, 2010.

Mai, C.: Atmospheric deposition of organic contaminants into the North Sea and the western Baltic Sea, PhD thesis, University of Hamburg, Hamburg, Germany, 444 pp., available at: http://ediss.sub.uni-hamburg.de/volltexte/2012/5771/, 2012.

Mandalakis, M., Tsapakis, M., Tsoga, A., and Stephanou, E. G.: Gas–particle concentrations and distribution of aliphatic hydrocarbons, PAHs, PCBs and PCDD/Fs in the atmosphere of Athens (Greece), Atmos. Environ., 36, 4023–4035, 2002.

Masclet, P., Pistikopoulos, P., Beyne, S., and Mouvier, G.: Long range transport and gas/particle distribution of polycyclic aromatic hydrocarbons at a remote site in the Mediterranean Sea, Atmos. Environ., 22, 639–650, 1988.

Pankow, J. F.: Review and comparative analysis of the the theory of partitioning between the gas and aerosol particulate phases in the atmosphere. Atmos. Environ., 21, 2275–2283, 1987.

Pankow, J. F. and Bidleman, T. F.: Interdependence of the slopes and intercepts from log-log correlations of measured gas-particle partitioning and vapor pressure, I. Theory and analysis of available data, Atmos. Environ., 26A, 1071–1080, 1992.

Pujo-Pay, M., Conan, P., Oriol, L., Cornet-Barthaux, V., Falco, C., Ghiglione, J.-F., Goyet, C., Moutin, T., and Prieur, L.: Integrated survey of elemental stoichiometry (C, N, P) from the western to eastern Mediterranean Sea, Biogeosciences, 8, 883–899, doi:10.5194/bg-8-883-2011, 2011.

Putaud, J. P., Raes, F., van Dingenen, R., Brüggemann, E., Facchini, M.C., Decesari, S., Fuzzi, S., Gehrig, R., Hüglin, C., Laj, P., Lorbeer, G., Maenhaut, W., Mihalopoulos, N., Müller, K., Querol, X., Rodriguez, S., Schneider, J., Spindler, G., ten Brink, H., Tørseth, K., and Wiedensohler, A.: A European aerosol phenomenology-2: chemical characteristics of particulate matter at kerbside, urban, rural and background sites in Europe, Atmos. Environ., 38, 2579–2595, 2004.

Qureshi, A., MacLeod, M., and Hungerbühler, K.: Modeling aerosol suspension from soils and oceans as sources of micropollutants to air, Chemosphere, 77, 495–500, 2009.

Ramdahl, T.: Retene – a molecular marker of wood combustion in ambient air. Nature, 306, 580–582, 1983.

Rowe, C. L., Mitchelmore, C. L., and Baker, J. E.: Lack of biological effects of water accommodated fractions of chemically-and physically-dispersed oil on molecular, physiological, and behavioral traits of juvenile snapping turtles following embryonic exposure, Sci. Total Environ., 407, 5344–5355, 2009.

Schmidl, C., Bauer, H., Dattler, A., Hitzenberger, R., and Weissenböck, G.: Chemical characterisation of particle emissions from burning leaves, Atmos. Environ., 42, 9070–9079, 2008.

Schnelle, J., Jänsch, J., Wolf, K., Gebefügi, I., and Kettrup, A.: Particle size dependent concentrations of polycyclic aromatic hydrocarbons (PAH) in the outdoor air, Chemosphere, 31, 3119–3127, 1995.

Schwarzenbach, R. P., Gschwend, P. M., and Imboden, D. M.: Environmental Organic Chemistry, 2nd ed., Wiley, Hoboken, USA, 906–937, 2003.

Spindler, G., Gnauk, T., Grüner, A., Iinuma, Y., Müller, K., Scheinhardt, S., and Herrmann, H.: Site-segregated characterization of PM_{10} at the EMEP site Melpitz (Germany) using a five-stage impactor: a six year study, J. Atmos. Chem., 69, 127–157, 2012.

Stohl, A., Hitzenberger, M., and Wotawa, G.: Validation of the Lagrangian particle dispersion model FLEXPART against large scale tracer experiments. Atmos. Environ., 32, 4245–4264, 1998.

Stohl, A., Forster, C., Eckhardt, S., Spichtinger, N., Huntrieser, H., Heland, J., Schlager, H.,Wilhelm, S., Arnold, F., and Cooper, O.: A backward modeling study of intercontinental pollution transport using aircraft measurements. J. Geophys. Res., 108, 4370, doi:10.1029/2002JD002862, 2003.

Stohl, A., Forster, C., Frank, A., Seibert, P., and Wotawa, G.: Technical note: The Lagrangian particle dispersion model FLEXPART version 6.2, Atmos. Chem. Phys., 5, 2461–2474, doi:10.5194/acp-5-2461-2005, 2005.

Tsapakis, M. and Stephanou, E. G.: Collection of gas and particle semi-volatile organic compounds: Use of an oxidant denuder to minimize polycyclic aromatic hydrocarbons degradation during high-volume air sampling, Atmos. Environ., 37, 4935–4944, 2003.

Tsapakis, M. and Stephanou, E. G.: Polycyclic aromatic hydrocarbons in the atmosphere of the Eastern Mediterranean, Environ. Sci. Technol., 39, 6584–6590, 2005a.

Tsapakis, M. and Stephanou, E. G.: Occurrence of gaseous and particulate polycyclic aromatic hydrocarbons in the urban atmosphere: study of sources and ambient temperature effect on the gas/particle concentration and distribution, Environ. Poll., 133, 147–156, 2005b.

Tsapakis, M., Stephanou, E. G., and Karakassis, I.: Evaluation of atmospheric transport as a non-point source of polycyclic aromatic hydrocarbons in marine sediments of the Eastern Mediterranean, Mar. Chem., 80, 283–298, 2003.

Tsapakis, M., Apostolaki, M., Eisenreich, S., and Stephanou, E. G.: Atmospheric deposition and marine sedimentation fluxes of polycyclic aromatic hydrocarbons in the Eastern Mediterranean Basin, Environ. Sci. Technol., 40, 4922–4927, 2006.

Woolf, D. K.: Bubbles and their role in gas exchange, in: Sea Surface and Global Change, edited by: Liss, P. S. and Duce, R. A., Cambridge University Press, Cambridge, UK, 173–206, 1997.

Zhong, G., Xie, Z., Möller, A., Halsall, C., Caba, A., Sturm, R., Tang, J., Zhang, G., and Ebinghaus, R.: Currently used pesticides, hexachlorobenzene and hexachlorocyclohexanes in the air and seawater of the German Bight (North Sea), Environ. Chem., 9, 405–414, 2012.